

**PREPARATION AND CHARACTERIZATION OF CARBON MOLECULAR
SIEVE MEMBRANE FROM POLYFURFURYL ALCOHOL**

By

WAN MOHD HAFIZ FAISAL BIN WAN HARUN

**Thesis submitted in fulfillment of the
requirement for the degree of
Master of Science**

July 2011

ACKNOWLEDGEMENTS

In the name of Allah, the Most Beneficent and the Most Merciful. All praises to Allah the Almighty for giving me the strength, guidance and patience in completing this thesis. First and foremost, I would like to express my deepest gratitude to my family for their endless love and support for me to pursue my MSc. degree. My deepest appreciation goes to Dr. Mohd Azmier Ahmad for serving as a successful supervisor of this research project. I would like to express my appreciation to my Co-Supervisor, Professor Dr. Abdul Latif Ahmad for his advice. Special credit also goes to the Dean of School of Chemical Engineering, Professor Dr. Azlina Harun @ Kamaruddin for their support in handling my postgraduate affairs. I would like to thank MOSTI for the ScienceFund grant (03-01-05-SF0418).

I would like to express my grateful thanks to Mr. Faiza, Mr. Shamsul Hidayat, Mrs. Latiffah and Mr. Abda Jamil for their technical guidance and support towards my experimental work. Besides, special thanks goes to postgraduate students; Azan, Behnam, Khalilah and Nurul for sharing their knowledge, professional advices and guidelines throughout the whole project. Useful discussions and suggestions from them are deeply appreciated. Last but not least, I would like to express deepest gratitude to those who have directly and indirectly contributed to the accomplishment and outcome of this project, especially my friends for their motivation, encouragement and moral support. Thank you so much.

***Wan Mohd Hafiz Faisal Wan Harun
July 2011***

TABLE OF CONTENTS

ACKNOWLEDGEMENTS	ii
TABLE OF CONTENTS	iii
LIST OF TABLES	vii
LIST OF FIGURES	ix
LIST OF PLATES	xii
LIST OF SYMBOLS	xiii
LIST OF ABBREVIATIONS	xv
ABSTRAK	xvii
ABSTRACT	xviii
CHAPTER ONE: INTRODUCTION	1
1.1 Overview of gas separation technology	1
1.2 Membrane technology for gas separation	3
1.3 Carbon molecular sieve membrane	5
1.4 Problem statement	7
1.5 Objectives of the research	8
1.6 Organization of the thesis	8
CHAPTER TWO: LITERATURE REVIEW	10
2.1 Membrane overview	10
2.2 Carbon molecular sieve membrane	12
2.3 Transport mechanism of gas in CMS membrane	15
2.3.1 Molecular sieving	15

2.3.2	Surface diffusion	16
2.3.3	Knudsen diffusion	17
2.4	CMS membrane development	18
2.4.1	Support	18
2.4.2	Intermediate layer	19
2.4.2.1	Sol gel	19
2.4.2.2	Organic additive	21
2.4.2.3	Drying and sintering	22
2.4.3	Carbon film	24
2.4.3.1	Precursor	24
2.4.3.2	Carbonization	28
2.5	CMS membrane characteristic	29
2.5.1	Effect of sintering temperature	29
2.5.2	Effect of carbonization temperature	30
2.5.3	Effect of thermal soak time	33
2.6	Gas permeability test	34
2.7	Design of experiment	36
2.7.1	Response surface methodology	37
2.7.2	Central composite design	38
2.7.3	Analysis of the data	40
CHAPTER THREE: MATERIALS AND METHODS		43
3.1	Materials	43
3.2	Experimental procedure	44

3.2.1	Preparation of substrate	44
3.2.3	Preparation of membrane layer	45
3.2.3.1	Polymerization	45
3.2.3.2	Carbonization	45
3.2.4	Characterization	47
3.2.4.1	X-Ray diffraction	47
3.2.4.2	Nitrogen adsorption-desorption	48
3.2.4.3	Fourier transform infra-red	48
3.2.4.4	Elemental analysis	48
3.2.4.5	Transmission electron microscopy	49
3.2.5	Gas permeability test	49
3.2.6	Experimental flow chart	52
3.2.7	Experimental design	54

CHAPTER FOUR: RESULTS AND DISCUSSIONS 57

4.1	Characteristics of substrate	57
4.2	Characteristics of membrane layer	59
4.2.1	Effect of carbonization temperature	59
4.2.2	Effect of thermal soak time	71
4.3	Experimental design	81
4.3.1	Development of empirical model equation for CMS membrane preparation	83
4.3.2	Effect of single process variable	87

4.3.2.1	Carbonization temperature	88
4.3.2.2	Thermal soak time	89
4.3.3	Optimization of preparation parameters	90
4.3.4	Characterization of optimized CMS membrane	91
CHAPTER FIVE: CONCLUSION AND RECOMMENDATION		95
5.1	Conclusion	95
5.2	Recommendation	96
REFERENCES		97
APPENDICES		106
Appendix A	Preparation of titania disk	106
Appendix B	Effect of curing time	107
Appendix C	Calculation of permeance and permselectivity	108
Appendix D	Calculation of d-spacing	109
Appendix E	Calculation of activation energy, E_p from Arrhenius equation	110

LIST OF TABLES

Table 1.1	Comparison of gas separation processes	3
Table 2.1	Membrane support and configuration	19
Table 2.2	Titania precursor and organic additive	21
Table 2.3	Maximum allowable ceramic thickness under given conditions	22
Table 2.4	CMS membrane precursor and the modification	25
Table 2.5	Properties of furfuryl alcohol	26
Table 2.6	Gas separation data for phenolic resin derived-carbon membranes obtained at 700°C by using different thermal soak time (Centeno et al., 2004)	34
Table 2.7	Central composite design (Tobias and Trutna, 2006)	39
Table 3.1	List of chemicals	43
Table 3.2	List of gases	44
Table 3.3	Sintering temperature for membrane substrate	45
Table 3.4	Independent variables and their coded levels for the central composite design	54
Table 3.5	Experimental design matrix	55
Table 4.1	Characteristics of substrate prepared at different sintering temperature	58
Table 4.2	d-spacing value of CMS membrane prepared at different carbonization temperature	60
Table 4.3	Pore characteristic of CMS membrane prepared at different carbonization temperature	65

Table 4.4	Activation energy of gas permeance at different carbonization temperature	70
Table 4.5	d-spacing value of CMS membrane prepared at different thermal soak time	72
Table 4.6	Pore characteristic of CMS membrane prepared at different thermal soak time	76
Table 4.7	Activation energy of gas permeance at different thermal soak time	80
Table 4.8	Design matrix with coded and actual level of variable and experimental responses value	82
Table 4.9	ANOVA for response surface linear model for O ₂ permeance of CMS membrane	85
Table 4.10	ANOVA for response surface linear model for O ₂ /N ₂ permselectivity of CMS membrane	85
Table 4.11	ANOVA for response surface linear model for CO ₂ permeance of CMS membrane	85
Table 4.12	ANOVA for response surface linear model for CO ₂ /CH ₄ permselectivity of CMS membrane	85
Table 4.13	Model validation for CMS membrane	91
Table 4.14	Predicted and actual result of gas permeance and permselectivity for optimized CMS membrane	91
Table B1	T _g value of PFA at different curing time	107

LIST OF FIGURES

Figure 2.1	Schematic diagram of a membrane separation process	10
Figure 2.2	Illustration of non-graphitize carbon; (a) HRTEM image and (b) Franklin's structure model (McEnaney, 1999).	12
Figure 2.3	Illustration of non-graphitize carbon or turbostratic carbon, that consist of four turbostratically layered sheets (Smith et al., 2004).	13
Figure 2.4	Illustration of idealized structure of slit pore in CMS membrane (Steel and Koros, 2003).	14
Figure 2.5	Mechanism of molecule transport in CMS membrane (Shekhawat et al., 2003)	15
Figure 2.6	Schematic diagram of the neck formation during initial step of sintering	23
Figure 2.7	Illustration of furfuryl alcohol polymerization (Belgacem and Gandini, 2008).	26
Figure 2.8	Formation of conjugated sequences during polymerization of furfuryl alcohol (Belgacem and Gandini, 2008).	27
Figure 2.9	Diel-Alder mechanism of the conjugated polymer sequences (Belgacem and Gandini, 2008).	28
Figure 2.10	Illustration of glassy carbon structure model (Dresselhaus et al., 1996).	32
Figure 2.11	Three type of central composite design (Halim, 2008)	40
Figure 3.1	The carbonization experimental set up	47
Figure 3.2	Schematic diagram of asymmetric CMS membrane	47
Figure 3.3	Experiment rig for single permeability test of CMS membrane	50
Figure 3.4	Illustration of permeation cell	51
Figure 3.5	Schematic flow diagram of experimental activities	53

Figure 4.1	Diffraction pattern of substrate prepared at different sintering temperature	57
Figure 4.2	Diffraction pattern of CMS membranes prepared at different carbonization temperature	60
Figure 4.3	FTIR spectrums of CMS membranes prepared at different carbonization temperature	62
Figure 4.4	[O]/[C] and [H]/[C] atomic ratio of CMS membrane prepared at different carbonization temperature	63
Figure 4.5	Isotherm plot of CMS membrane prepared at different carbonization temperature	64
Figure 4.6	Pore size distribution of CMS membrane prepared at different carbonization temperature	65
Figure 4.7	Gas permeances at room temperature of CMS membranes prepared at different carbonization temperature	66
Figure 4.8	Gas permeances at different permeation temperature	67
Figure 4.9	Ideal selectivities of gas pairs at different permeation temperature (a) O ₂ /N ₂ (b) CO ₂ /CH ₄	68
Figure 4.10	Arrhenius plot of CMS membrane prepared at different carbonization temperature; (a) CMS400, (b) CMS500 and (c) CMS600	69
Figure 4.11	Diffraction pattern of CMS membrane prepared at different thermal soak time	71
Figure 4.12	FTIR spectrums of CMS membranes prepared at different thermal soak time	73
Figure 4.13	[O]/[C] and [H]/[C] atomic ratio of CMS membrane prepared at different thermal soak time	74
Figure 4.14	Isotherm plot of CMS membrane prepared at different thermal soak time	74

Figure 4.15	Pore size distribution of CMS membrane prepared at different thermal soak time	75
Figure 4.16	Gas permeances at room temperature of CMS membranes prepared at different thermal soak time	77
Figure 4.17	Gas permeances at different permeation temperature; (a) O ₂ , (b) N ₂ , (c) CO ₂ and (d) CH ₄	78
Figure 4.18	Ideal selectivity of gas pairs at different permeation temperature (a) O ₂ /N ₂ (b) CO ₂ /CH ₄	79
Figure 4.19	Arrhenius plot of CMS membranes prepared at different thermal soak time; (a) CMS1h, (b) CMS2h, (c) CMS3h and (d) CMS4h	80
Figure 4.20	Predicted value versus experimental value of O ₂ permeance	86
Figure 4.21	Predicted value versus experimental value of O ₂ /N ₂ ideal selectivity	86
Figure 4.22	Predicted value versus experimental value of CO ₂ permeance	87
Figure 4.23	Predicted value versus experimental value of CO ₂ /CH ₄ ideal selectivity	87
Figure 4.24	Individual effect of carbonization temperature: (a) O ₂ permeance, (b) O ₂ /N ₂ ideal selectivity, (c) CO ₂ permeance and (d) CO ₂ /CH ₄ ideal selectivity ($x_2=2.50$ hours)	89
Figure 4.25	Individual effect of thermal soak time: (a) O ₂ permeance, (b) O ₂ /N ₂ ideal selectivity, (c) CO ₂ permeance and (d) CO ₂ /CH ₄ ideal selectivity ($x_1=500^\circ\text{C}$)	90
Figure 4.26	XRD pattern of optimized CMS membrane	92
Figure 4.27	FTIR spectrum of the optimized CMS membrane	93

LIST OF PLATES

Plate 3.1	Wire wound tube furnace	46
Plate 4.1	Morphology of optimized CMS membrane by EFTEM	94
Plate A	(a) Stainless steel mould and (b) Hydraulic hand pump	106

LIST OF SYMBOLS

A	Adsorption potential	
D	Diffusion coefficient	m^2/s
d_C	Ultramicropore dimension	nm
d_{TV}	Size of adsorptive micropore	nm
d_λ	Jump length nm	
E_d	Activation energy of diffusion	kJ/mol
E_P	Activation energy of permeation	kJ/mol
l	Membrane thickness	m
L_C	Crystallite size	nm
N	Total number of experiments required	-
N_A	Gas molar flow rate of species A	mol/s
p_o	Saturation pressure	bar
P_O	Temperature dependant constant	-
P_A	Gas permeability of species A	$cm^3 \cdot mm / (m^2 \cdot bar \cdot s)$
p_{rel}	Relative pressure	bar
Q_A	Gas permeance of species A	$mol/m^2 \cdot s \cdot Pa$
R	Universal gas constant	8.314 J/mol.K
R^2	Correlation coefficient	-
S	Sorption coefficient	
T_g	Glass transition temperature	$^{\circ}C$
V_T	Total pore volume	cm^3/g
W_o	Weight of adsorbate	g
x	Statistical parameter	-
Y	Predicted response	-

Greek letters

α	Permselectivity	-
β	Affinity coefficient	-
θ	Bragg's angle	°
ΔC	Concentration gradient	mol/cm ³
ΔE	Electrical potential gradient	V/m
ΔH_{ads}	Heat of adsorption	kJ
ΔP	Pressure drop	Pa
ΔT	Temperature gradient	K
λ	Wavelength nm	

LIST OF ABBREVIATIONS

AFM	Atomic force microscopic
ANOVA	Analysis of variance
BET	Brunauer-Emmett-Teller
BJH	Barret-Joyner-Halenda
BPDA-ODA	2, 3, 3', 4'-biphenyl tetracarboxylic dianhydride- 4, 4'-oxydianiline
CCD	Central composite design
CMS	Carbon molecular sieve
CVD	Chemical vapor deposition
DMA	Dynamic mechanical analysis
DR	Dubinín-Radushkevich
DSC	Differential scanning calorimetry
EA	Elemental analysis
FA	Furfuryl alcohol
FTIR	Fourier transform infrared
FWHM	Full width at half maximum
HK	Horvath-Kawazoe
HPC	Hydroxy-propyl cellulose
IL	Intermediate layer
IR	Infrared
IUPAC	International Union of Pure and Applied Chemistry
PAN	Polyacrylonitrile
PEI	Polyetherimide
PFA	Polyfurfuryl alcohol
PSA	Pressure swing adsorption

PTFE	Poly-tetrafluoro ethylene
PVA	Polyvinyl alcohol
PVDC	Polyvinylidene chloride
RSM	Response surface methodology
SEM	Scanning electron microscopy
STM	Scanning tunneling microscope
TEM	Transmission electron microscopy
TGA	Thernogravimetric analysis
TTIP	Titanium iso-propoxide
VSA	Volume swing adsorption
XRD	X-ray diffraction

PENYEDIAAN DAN PENCIRIAN MEMBRAN TAPISAN MOLEKULAR KARBON DARIPADA POLIFURFURIL ALKOHOL

ABSTRAK

Penggunaan membran tak organik dapat meminimumkan masalah-masalah yang dihadapi oleh teknologi-teknologi pemisah gas tradisional seperti penjerapan, proses kimia dan membran polimer. Dalam kajian ini, membran tapisan molekular karbon telah berjaya disediakan daripada polifurfuril alkohol. Substrat membran tapisan molekular karbon telah disediakan dengan menyalut cecair titania pada cakera titania dan dipanaskan pada suhu pembakaran antara 300 hingga 600°C. Dalam pada itu, filem karbon telah dihasilkan dengan mencelup substrat kepada cecair polifurfuril alkohol diikuti dengan pengkarbonan pada suhu antara 400 hingga 600°C selama 1 hingga 4 jam tempoh rendam termal. Purata saiz liang dan ruang-d masing-masing berkurang kepada 4.72Å and 3.67Å apabila suhu pengkarbonan meningkat sehingga 600°C. Dalam pada itu, analisis muktamat mengesahkan pengkarbonan pada 600°C menyebabkan penurunan sebanyak 41% dan 87% masing-masing terhadap nisbah [H]/[C] dan [O]/[C]. Analisis varian menunjukkan suhu pengkarbonan menunjukkan kesan yang signifikan kepada peresapan gas dan kepemilihan unggul berbanding tempoh rendam termal. Keadaan penyediaan membran tapisan molekular karbon diperoleh pada suhu dan tempoh pemanasan 600°C dan 4 jam. Ciri-ciri peresapan gas adalah 4.95×10^{-8} mol/m².s.Pa, 7.74×10^{-8} mol/m².s.Pa, 1.82 dan 5.31 masing-masing kepada resapan O₂, resapan CO₂, kepemilihan unggul O₂/N₂ dan CO₂/CH₄. Membran tapisan molecular karbon optimum menunjukkan peresapan gas dan kepemilihan unggul tertinggi.

PREPARATION AND CHARACTERIZATION OF CARBON MOLECULAR SIEVE MEMBRANE FROM POLYFURFURYL ALCOHOL

ABSTRACT

The application of inorganic membrane would minimize the problems suffered by conventional gas separation technologies such as adsorption, chemical process and polymeric membrane. In this work carbon molecular sieve (CMS) membranes were successfully prepared from polyfurfuryl alcohol (PFA). The CMS membrane substrate was prepared first by coating the dope solution of titania sol onto the titania disk and heated from 300 to 600°C of sintering temperature. On the other hand, the carbon film was formed by dipping the substrate onto PFA solution followed by carbonization between 400 to 600°C for 1 to 4 hours of thermal soak times. The average pore size and d-spacing were reduced to 4.72Å and 3.67Å, respectively as the carbonization temperature increase up to 600°C. On the other hand, the elemental analysis verified that the carbonization at 600°C induce 41% and 87% percentage reduction of [H]/[C] and [O]/[C] ratios, respectively. The analysis of variance reveal the carbonization temperature exhibits significant effect on gas permeances and ideal selectivity compared to thermal soak time. The optimum CMS membrane preparation conditions were obtained at 600°C and 4 hours of carbonization temperature and thermal soak time, respectively. The permeation properties of the optimum CMS membrane were 4.95×10^{-8} mol/m².s.Pa, 7.74×10^{-8} mol/m².s.Pa, 1.82 and 5.31 for O₂ permeance, CO₂ permeance, O₂/N₂ ideal selectivity and CO₂/CH₄ ideal selectivity respectively. The optimum CMS membrane possesses the highest gas permeance and ideal selectivity.

CHAPTER ONE

INTRODUCTION

1.1 Overview of gas separation technology

Every year, a hundred million tons of pure oxygen are produced to meet the demand and caused the gas to be the top five in the production of commodity chemical in the world (Hashim et al., 2010). The large production was contributed by the wide applications of the oxygen in power generation and the production of steel and chemicals such as ethylene oxide, ethylene dichloride, acetic acid, etc. High demand of oxygen induced the high price of the commodity, where the price was reported to be USD\$0.21/kg in 2001.

In general, water and air are the main sources for oxygen, where the separation and purification processing would generate pure oxygen. Nowadays, the mass production of pure oxygen is based on the separation of air, which involved two separation techniques; cryogenic and non-cryogenic. The cryogenic is matured and well developed technique, where 15 000 tons of high purity of oxygen (>99% purity) could be produced daily (Bose, 2008). However this technology required super-cooled temperature during separation process. The instalment of chillers to provide suitable condition for separation process would increase the capital and utility cost in operation. In addition, the requirement of large site and long start-up hindered the efficiency of this technology in industrial point of view.

Meanwhile, non-cryogenic technique is divided into several technologies such as adsorption, chemical process and polymeric membrane. Pressure swing adsorption (PSA) and vacuum swing adsorption (VSA) are the examples of the adsorption technologies which applying zeolite adsorbent bed. These technologies selectively

adsorb nitrogen from the air and discharged pure oxygen as the product. Usually, 1500 Nm³ per hour of oxygen (90-94% purity) could be produced by the adsorption technology. In 1990, Air Product and Chemicals (Ltd.) operated a small-scale pilot unit of molten salt chemical process, which is called MOLTOXTM. This technology performed separation of oxygen from air by circulation of molten salt, where manipulation of temperature and pressure of the molten salt stream may control the absorption and desorption of oxygen. This technology reported to generate high purity of oxygen gas (99.9% purity) (Smith and Klosek, 2001).

Recently, a new kind of non-cryogenic technology which is called ion transport membrane (ITM) was emerged as an alternative technology to generate oxygen from air. The separation process of this membrane was carried out at 800-900°C of permeation temperature (Hashim et al., 2010). The separation mechanism was based on the ionic conversion, where the oxygen molecules were converted to oxygen ions at the surface of the membrane. Then the ions transported through the membrane and the oxygen molecules reformed after passing through the membrane material (Smith and Klosek, 2001). Similar to non-cryogenic, cryogenic technologies required instalment of various equipments for operating process, such as the vacuum system and heating system for regeneration of the adsorbent and separation operation, respectively. This would increase the capital and utility cost which could reduce the margin industry.

Besides oxygen, the methane which is the major constituent of natural gas is also considered as a high value commodity due to low emission of greenhouse gas. The market of the gas is growing rapidly where the global consumption of methane is projected to increase from 95 trillion cubic feet in 2003 to 182 trillion cubic feet in 2030 (Xiao et al., 2009). Thus the increase of natural gas production is essentially

important to meet the global demand. Usually, the crude natural gas contains carbon dioxide gas; where the content is vary from 4 to 50 mol %. The acidic characteristic of carbon dioxide may causes several impacts such as reduction of fuel heating value, large volume of gas for transportation and storage, pipeline corrosion and pollution to the atmosphere. Thus the crude natural gas must be pre-processes so as to meet the typical specification of 2 to 5 mol % of carbon dioxide content in the pipeline (Hao et al., 2002).

Alkanolamine solution and PSA technologies are considered matured technologies for separating the carbon dioxide from natural gas (Datta and Sen, 2006). Despite the maturity and developing status of the separation and purification technology of methane, they basically suffered from various problems. The PSA possesses high utility cost where regeneration of bed required low pressure condition to reduce nitrogen holding capacity of the adsorbent (Datta and Sen, 2006). In addition, the PSA technology is well known to cause noise pollution and required high cost for equipment maintenance. The combination of salt and oxygen facilitates the corrosion of the molten salt chemical process facility and lead to high capital cost while the ITM and alkanolamine solution treatment require gas-to-liquid phase change and solvent regeneration that increase the operating cost (Smith and Klosek, 2001). Thus the application of alternative technology for oxygen and methane separation is required to overcome the problems.

1.2 Membrane technology for gas separation

The application of membrane technology for gas separation was started in the early 1980s. In particular, the membrane technology possesses low capital and operating cost, simplicity of operation, better utilization of space and environmental

friendly (Xiao et al., 2009). In addition, membrane gas separation unit have no moving component parts, thus ensuring the exceptional reliability of the product. However the semi-mature status of the membrane technology cause the gas purity limited to 40% by volume (Hashim et al., 2011). Thus membrane technology may appear advantageous for small-to-medium scale operations and non-stringent product purity requirements.

Generally, polymers are used as the conventional materials for membrane production. The membrane is dense and permits specific gas to pass throughout the membrane by solution-diffusion mechanism (Gupta et al., 2006). Commonly, the glassy polymer is chosen as the precursor of the membrane due to high transition glass temperature and amorphous nature of the polymer. The glassy polymer offers high loading bearing which allows for high pressure drop across the membrane and enables the membrane to act as the selective layer and support. Besides, the glassy polymer offers a more structured sieving matrix than the rubbery polymer, thus performing separation of gas pairs by size selective sieving mechanism (Robeson, 1999). However there still present significant segmental motions in glassy polymers which limiting the performance of polymeric membrane (Singh-Ghosal and Koros, 2000).

The separation performance of polymeric membrane process is described by the selectivity and permeability. These two properties appear to be inversely related, that is if the permeability for a species increase, the corresponding selectivity tends to decrease. There appears to be an upper bound for the performance of the membrane (Robeson et al., 1994). The long-term performance of polymer membrane is hindered by plasticization, which results from the penetration of condensable gas such as CO₂. The CO₂ gas causes swelling of the polymer matrix and reduces the interaction

between the adjacent segments of polymer chains, consequently increasing the segmental mobility and free volume. As a result an increase in permeability and loss in selectivity is observed (Dong et al., 2010). Due to the shortcoming of the polymer membrane, versatile inorganic membrane emerged as the solution to overcome those problems. Recent article reported the perovskite based membrane capable to perform oxidation separation from air at 700°C of operation temperature (Ahmad et al., 2011). In addition, no change on pore diameter of inorganic membrane after exposure of acidic solution by Burggraaf and co-worker (1996) verified the inorganic membranes inherently more chemically stable than polymeric membrane. Thus synthesis and application of inorganic membrane is a potential research work to improve the quality and process operation of gas enriched product.

1.3 Carbon molecular sieve membrane

In recent years, researchers have produced carbon molecular sieve (CMS) membrane by carbonization of polymeric precursors. Typically, improved selectivities for O₂/N₂ and CO₂/CH₄ were observed and subsequently bring the higher purity of end product. CMS membrane performs gas transportation by sorption-diffusion mechanism (Singh-Ghosal and Koros, 2000).

Generally, the CMS membrane is produced as asymmetric membrane, where the bottom layer is useful in providing mechanical strength to the membrane due the brittle nature suffered by carbonized material (Saufi and Ismail, 2004). The bottom layer is called substrate and usually made from ceramic material, which can withstand high temperature during carbonization treatment. Commonly the surface of the substrate provides smooth layer with pore size lies in the mesopore region. Meanwhile the carbon layer on the top of the CMS membrane consists of

ultramicro-pore and micro-pore which is responsible for gas selective and diffusion, respectively. The typical effective pore diameter of CMS membrane is between 0.3 to 1.0 nm which is comparable with the size of the gas molecules being separated (Fuertes and Centeno, 1998).

Typically, the carbonization treatment and type of precursor are the main factors in determine the pore size of CMS membrane (Saufi and Ismail, 2004). Carbonization must be carried out at suitable temperature to trigger the formation of micro-pore. Insufficient temperature leads to less permeance due to low pore volume. Meanwhile, to high of carbonization temperature lead to development of glassy carbon which contributes to low gas permeance due to densification of carbon material. During carbonization, the chemical substances in dense polymer matrix were evolved and cause channelling of the matrix. The pore volume started to develop and cause the porosity to increase (Guigo et al., 2009).

The selection of precursor is a crucial factor in producing CMS membrane. It is common to use thermosetting polymer as the precursor due to its thermal stability. Thermosetting polymer consists of crosslink network which could resist graphitization during carbonization. Instead of that, non-graphitize or disordered carbon will form after carbonization (Burket et al., 2008). Non-graphitize carbon exhibits high porosity with small opening of slit-shape pore, which permits only small gas to enter. The properties of the pores are dependent on the type of thermosetting polymer. The selection of high degree crosslink of thermosetting polymer contribute to formation of large carbon content after carbonization, which indicate the large amount of pore volume in CMS membrane. The common thermosetting polymers are polyimide (Kim et al., 2004), phenolic resin (Centeno et

al., 2004), cellulose (Soffer and Koresh, 1983) and polyetherimide (Salleh and Ismail, 2011).

1.4 Problem statement

Currently cryogenic technique becomes the mature and developed technology in gas separation process. This technology is capable to provide high purity gas at large volume. However this technology involves high utility cost due to the requirement of extremely low temperature for gas separation. This situation triggers the developments of alternative technology such as polymeric membrane which consume less utility cost. Polymeric membranes are used in practical industrial applications as they have reproducible processibility and reasonable gas selectivity. However, current polymeric membrane materials have reached a limit in their productivity-selectivity trade-off relationship and difficult to achieve significant improvement. Besides, polymeric membranes cannot operate in corrosive and high temperature environments.

To overcome these limitations, the usage of rigid and nonreactive materials as a membrane precursor, bring the membrane application towards the harsh environment with the combination of superior permeance-selectivity. The inorganic membranes are usually exhibits high performance compared to polymeric membrane. One of the attractive inorganic membranes is CMS membrane. The capability of CMS membrane to surpass the limit of polymeric membrane has brought much interest for research and development. CMS membranes possess high rigidity and inert structure, which retain the stability in harsh environment. In this work, CMS membranes were prepared from thermosetting polymer of polyfurfuryl alcohol (PFA) which is thermally stable and possesses high glass transition temperature. The

structure of PFA is rigid due to the crosslinked structure, which will hinder the melting of polymer matrix during carbonization and contribute to high carbon yield.

1.5 Objectives of the research

The objectives of the research are as follow:

- i. To study the physical changes of the substrate at various sintering temperature.
- ii. To characterize and evaluate the ideal gas permeation of O₂, N₂, CO₂ and CH₄ for CMS membrane at different carbonization temperature and thermal soak time.
- iii. To determine the ideal selectivity of O₂/N₂ and CO₂/CH₄ gas pairs on each membrane sample at different permeation temperature.
- iv. To optimize the CMS membrane preparation conditions by using response surface methodology.

1.6 Organization of the thesis

Chapter one presents the current scenario of gases separation and purification process. The discussions consider the supply and demand of the commodity and the problem suffered by the conventional technologies. Problem statement, objectives and the organization of the thesis are also highlighted.

Chapter two present the literature review which cover the general information regarding classification of the membrane, followed by the literature review on the background of CMS membrane and the gas transport mechanism which possesses by the CMS membrane. In addition, an overview of various support, polymer precursors and intermediate layer precursor are provided in this chapter.

Chapter three present the list of the chemical and equipments used in the present research work. The experimental procedure consisting of sol-gel production, polymerization, carbonization, characterization, permeability test, model fitting and statistical analysis. It is followed with the schematic flow diagram showing the overall activities carried out in this research.

Chapter four present the experimental result for variation of sintering temperature, carbonization temperature and thermal soak time. It is followed by the regression model equation developed, together with the optimization result based on the permeance and ideal selectivity of gases. Then, it followed the characterization of the optimized CMS membrane.

Chapter five present the conclusion that reflects the achievements of all the objectives which were obtained throughout the study as well as the recommendations for the future research. These recommendations offered the significance and importance related to the present research

CHAPTER TWO

LITERATURE REVIEW

2.1 Membrane overview

A membrane can be described as a selective thin barrier between two bulk phases that permits transport of some component and retain other. The membrane permeability indicates the rate at which a given component is transported through a membrane. The permeability is determined by the structure of the membrane, size of the permeating components and driving force. The driving forces are concentration (ΔC), pressure (ΔP) or electrical potential gradient (ΔE) across the membrane. Another characteristic property is the selectivity, which is the measure of the relative permeability of different components through the membrane. Ideally, a membrane with a high permeability and selectivity is required to meet high productivity.

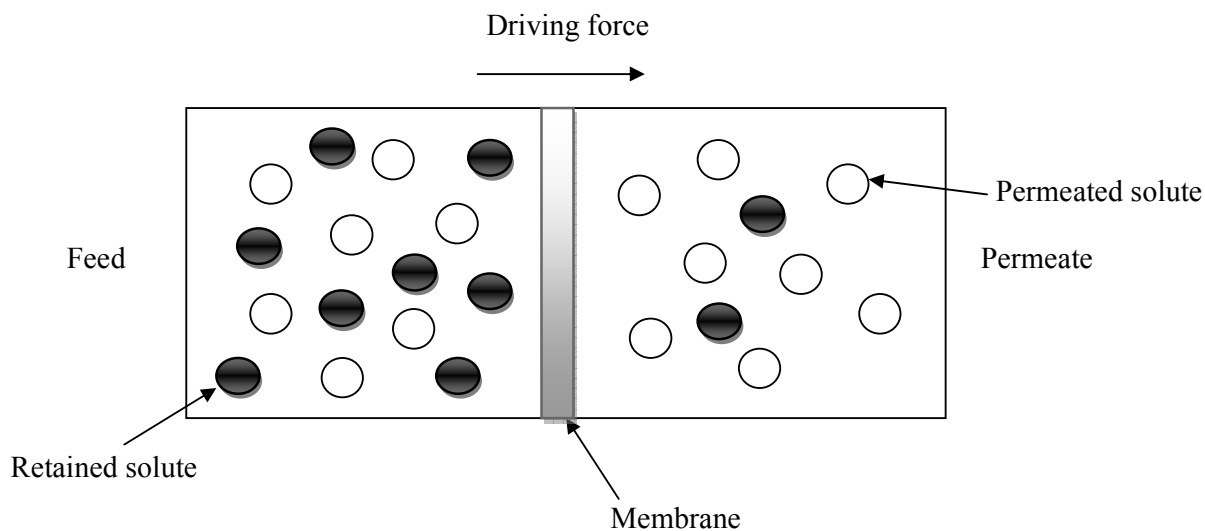


Figure 2.1 Schematic diagram of a membrane separation process.

The membrane can be classified according to different viewpoints. Basically it is classified based on the nature; biological and synthetic membrane. Biological

membrane takes place in the living organism while the latter is man-made. The synthetic membrane can be classified based on the material; organic and inorganic. Generally, the organic membrane is made from organic polymer while the latter is ceramic and metal. Membrane can also be classified based on structure and separation principles; porous and dense membrane. The porous membrane induces separation by discriminating between particle sizes. Meanwhile the dense membrane is used for separation of the same molecule size and performs separation through differences in solubility and differences in diffusivity. Basically, the separation characteristics of dense membrane are determined by the intrinsic properties of the membrane's material (Mulder, 1996).

The membrane also can be classified based on the morphology; asymmetric and symmetric. The asymmetrical membrane possesses two or more layers. Each layer exhibits different characteristic; the layer in the feed section exhibit smaller pore or dense and permits certain molecule to pass through, while the permeate section possesses larger pore and provide less resistance for molecule transportation (Mulder, 1996). The symmetrical membrane consists of single layer that exhibits the same characteristic for the whole section of membrane. Membrane also can be classified according to their pore size which is the distance between two opposite walls of the pore. The pore size determines the capability of the membrane to separate the particles with different size and dimension. Based on the International Union of Pure and Applied Chemistry (IUPAC) regulation, the pore size is divided into three regions; micropore (pore size $< 2\text{nm}$), mesopore ($2\text{nm} < \text{pore size} < 50\text{nm}$) and macropore (pore size $> 50\text{nm}$). Most of inorganic membrane for gas separation application contains pores in the microporous region such as carbon molecular sieve and zeolite membrane.

2.2 Carbon molecular sieve membrane

In recent years, researchers have produced carbon molecular sieve (CMS) membrane by carbonization of thermosetting polymeric precursors. The thermosetting polymer consists of crosslinked network and provides rigidity to the material. During carbonization, the crosslink property strengthens the polymer structure and prevents melting which is suffered by thermoplastic polymer (Saufi and Ismail, 2004). The crosslink structure also retards the graphitization of the thermosetting polymer and induce the formation of non-graphitize carbon. The non-graphitize carbon possesses amorphous characteristic, where the grapheme sheets are chaotically misalignment (Burket et al., 2007). Figure 2.2 illustrates the high-resolution transmission electron microscope (HRTEM) image and the Franklin's structure of non-graphitize carbon. The non-graphitize carbon possesses randomly oriented graphite crystallites and connected by disordered graphene sheet (McEnaney, 1999).

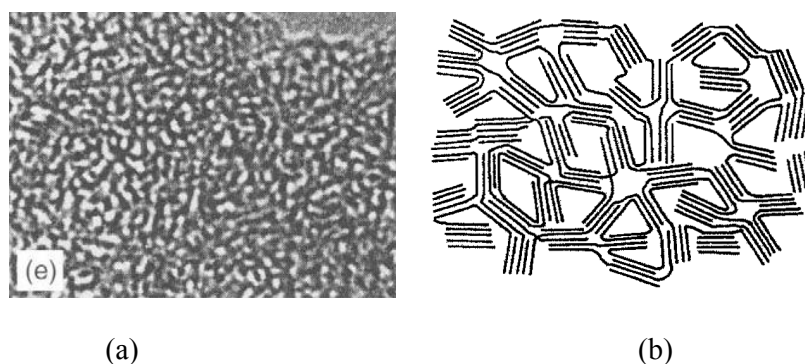


Figure 2.2 Illustration of non-graphitize carbon; (a) HRTEM image and (b) Franklin's structure model (McEnaney, 1999).

A model was demonstrated by simulation to create a three dimensional structure of non-graphitize carbon in CMS membrane. Basically, the graphene sheet

consists of five, six and seven-member rings. The non-hexagonal rings within the grapheme sheets generate the curvature of the structure. The curve grapheme sheets are turbostratically stacked into each other; where the complete stacked structure is typically consist of ten graphene sheets. The complete structure of non-graphitize carbon is also called turbostratic carbon. Figure 2.3 illustrates the model structure of non-graphitize carbon or turbostratic carbon (Smith et al., 2004). The curve nature of non-graphitize carbon induced the formation of slit pores in non-graphitize carbon (Chen et al., 2009). The pores are mostly in a range below 10 Å with the pore size distribution at an average of 5 Å, which fall in micropore region (Burket et al., 2008). The accessible micropores in the CMS membrane induce the gas separation by size exclusion, where it permits the small molecule while retains the big molecule.

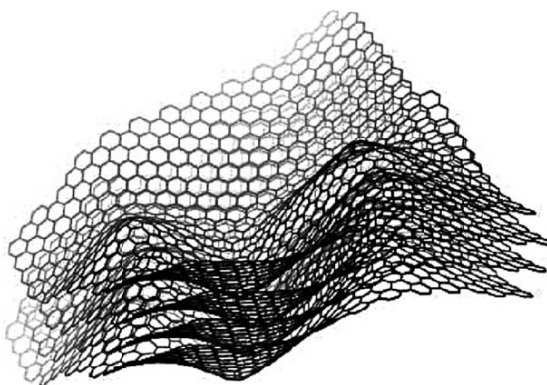


Figure 2.3 Illustration of non-graphitize carbon or turbostratic carbon, that consist of four turbostratically layered sheets (Smith et al., 2004).

In industrial point of view, CMS membranes should possess high productivity, which indicated by high flux of product. In the same time, the selectivity must be considered high and sufficient for gas enrichment purpose. Thus, the physical characteristic of CMS membrane; pore volume, pore width and pore size distribution, must be optimized or fine-tuned using modification steps. Various

modification steps have been listed by Saufi and Ismail (2004). The most reliable method is chemical vapour deposition (CVD), where the CMS membrane exposed to a vapor organic material such as propylene. This method could reduce the pore mouth or pore width, subsequently change the supermicropore to ultramicropore which possess 3 to 5 Å of pore width. In addition, the pore volume inside the channelling was not changed since the CVD only applied to the exposed surface. Thus, the increase of selectivity and maintained permeability were observed for the CVD treated CMS membrane. The opening of pore mouth for slit pore system can be illustrated by d_c in Figure 2.4.

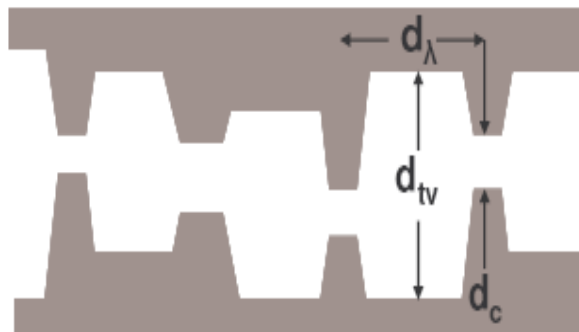


Figure 2.4 Illustration of idealized structure of slit pore in CMS membrane (Steel and Koros, 2003).

The d_λ is regarding to the dimension of effective diffusion jump length (λ), while the d_{tv} is regarding to the transverse dimension and d_c is the critical dimension of the ultramicropore. The d_c is responsible for molecular sieving discrimination of gases like oxygen and nitrogen, while the gas flux determined by d_{tv} and d_λ . Steel and Koros (2003) found that the d_λ , d_{tv} and d_c parameters shifted to a more compact structure as final carbonization temperature and thermal soak time increase.

2.3 Transport mechanism of gas in CMS membrane

The gas transport mechanism in CMS membrane is dependent on the pore size. There are four mechanisms were reported to occur for gas transportation in CMS membrane which were Knudsen diffusion, surface diffusion and molecular sieving (Salleh et al., 2011).

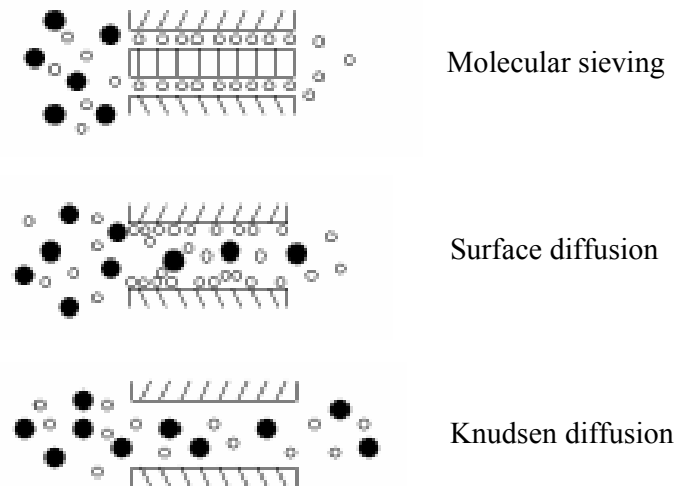


Figure 2.5 Mechanism of molecule transport in CMS membrane (Shekhawat et al., 2003)

2.3.1 Molecular sieving

Generally, the carbonization of thermosetting polymer produce pores in the size range from 0.3 nm to 0.8 nm. The wide distribution of pore size facilitates the combination of gas transport mechanism, since it is dependent on pore size. Gilron and Soffer (2002) affirm to use 0.5 to 2.0 nm as the cut-off between the molecular sieving and those operating by surface and Knudsen diffusion. Thus molecular sieving mechanism which is an activated process will be dominant for the smallest pore. Molecular sieving mechanism performs separation by exclusion of the molecule size, where it permits the passage of small molecules of a gas through the pores, and retains the large molecules (Saufi and Ismail, 2004). The transport

mechanism and the temperature dependence of the permeance for molecular sieving are listed in Equation 2.1 and 2.2, respectively.

$$D_{MS,c} = D_{MS}^0 \exp\left(\frac{-E_{a,MS}}{RT}\right) \quad (2.1)$$

$$F_{MS} \sim D_c(T) \exp\left\{\frac{-(E_{a,MS} - E_{ads})}{RT}\right\} \quad (2.2)$$

where $D_{MS,c}$ is the corrected diffusion coefficient with thermodynamic correction factor, D_{MS}^0 is the diffusion coefficient, $E_{a,MS}$ is the transport activation energy, F_{MS} is the gas permeance, R is the universal gas constant, T is the permeation temperature and E_{ads} is the heat of adsorption. The transport in molecular sieving is increase with permeation temperature as the activation energy is higher than heat of adsorption (Anderson et al., 2008).

2.3.2 Surface diffusion

Surface diffusion is an activated process and dominates for pores possess three times larger than the diffusing gas. This transport considered the affinity between the gas components and the membrane, where the polar gas molecules are selectively adsorbed onto the membrane surface and transport across the surface in the direction of decreasing surface concentration (Barsema et al., 2004). The adsorbed species on the membrane pores reduce the size of accessible void space throughout the pore and eliminate the transport of non-selective molecule. Beside the nature of the membrane surface, the concentration of the adsorbed species depends upon the temperature and pressure of the gas. The transport mechanism and the temperature dependence of the permeance for surface diffusion are listed in Equation 2.3 and 2.4, respectively.

$$D_{S,c} = D_S^0 \exp\left(\frac{-E_{a,S}}{RT}\right) \quad (2.3)$$

$$F_S \sim D_O(T) \exp\left\{\frac{-(E_{a,S}-E_{ads})}{RT}\right\} \quad (2.4)$$

where $D_{S,c}$ is the corrected diffusion coefficient with thermodynamic correction factor, D_S^0 is the diffusion coefficient, $E_{a,S}$ is the transport activation energy and F_S is the gas permeance for surface diffusion transport. The effect of permeation temperature in surface diffusion transport influence by the value of activation energy difference. The activation energy difference, $\Delta E_S = E_{a,S} - E_{ads}$ may be positive or negative, depend on the relative values of $E_{a,S}$ and E_{ads} . When $\Delta E_S < 0$, gas transport will decrease with permeation temperature while $\Delta E_S > 0$ induce the gas transport increase with permeation temperature (Gilron and Soffer, 2002).

2.3.3 Knudsen diffusion

The widest pore size facilitates the Knudsen diffusion in gas transportation (Gilron and Soffer, 2002). This mechanism identified for pores possess diameters smaller than the mean free path of the gas molecules. As a result, the movement of molecules inside the narrow pore channels takes place through collisions of the diffusing molecules with the surface wall rather than with each other (Shekhawat et al., 2003). The transport equation and the temperature dependence of the permeance for Knudsen diffusion are listed in Equation 2.5 and 2.6, respectively.

$$D_{K,c} = \frac{d_p}{3} \sqrt{\frac{8RT}{\pi M}} \quad (2.5)$$

$$F_K \sim (MRT)^{-0.5} \quad (2.6)$$

where $D_{K,c}$ is the corrected diffusion coefficient with thermodynamic correction factor, M is the gas molecular weight and F_K is the gas permeance. Based on Equation 2.5, Knudsen diffusivity possesses inverse relationship with the molecular weight of the gas, where high molecular weight induces low gas diffusivity.

2.4 CMS membrane development

Development of CMS membrane involved the preparation of support, intermediate layer and carbon layer.

2.4.1 Support

The CMS membrane is usually produced as supported membrane, where it is useful to provide mechanical strength to the carbon layer, increase the thermal stability of the membrane and reduces the tensile stress during sintering process (Mallada and Menéndez, 2008). Besides, the supported CMS membrane also has the advantage of being available in various configurations such as flat plates, tube and disk, which can be used depending on the requirements of the particular applications. Usually, the support is made by ceramic materials, where the sintering process may control the pore size of the support. Typically, the pore sizes in the support are from 0.1 to 100 μ m (Foley et al., 1999). Table 2.1 shows the list of the material of the support and the CMS membrane configuration used by previous researches.

Table 2.1: Membrane support and configuration.

Material	Average pore diameter (μm)	Membrane configuration	References
α -alumina	0.14	Disk	Zhou et al, 2003
α -alumina	0.15	Tubular	Park et al, 2004
α -alumina	0.14	Tubular	Kusakabe et al, 1998
α -alumina	0.14	Tubular	Kita et al, 2006
Aluminium oxide	0.02	Disk	Wang and Hong, 2005
Stainless steel	0.20	Tubular	Shiflett and Foley, 2000
Stainless steel	0.20	Disk	Acharya and Foley, 1999
Graphite	0.70	Disk	Rao and Sircar, 1996
Graphite and phenolic resin	1.00	Disk	Fuertes and Centeno, 1998
Phenol formaldehyde	na	Tubular	Zhang et al, 2006

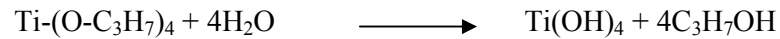
2.4.2 Intermediate layer

Generally, the support possesses large pores and high surface roughness which lead to diffusion of polymer (molecular sieve layer precursor) into the support. This problem is solved by deposition of intermediate layer onto the surface of the support. The preparation of intermediate layer involves several steps, such as preparation of sol gel, preparation of organic additive for the sol, drying and sintering.

2.4.2.1 Sol gel

A sol is defined as a stable suspension of colloidal particles within a liquid. The preparation of sol from sol-gel techniques can be applied to produce the intermediate layer of CMS membrane. The sol can be prepared by hydrolysis and condensation of alkoxides. This technique is capable to produce high-purity, ultrafine

and nano-scale particles by manipulation of certain parameters during preparation (Zaspalis et al., 1992). For titania sol production, titanium tetra-isopropoxide (TTIP) is commonly used as the precursor. The hydrolysis of TTIP may be considered as follows:



In this process, the molecular precursor is titanium which is metal alkoxide. It is bound by organic ligands to the central metal or metal ion. Colloidal particles are submitted to Brownian motion in a liquid medium. These particles collide each other and induce the occurrence of two phenomena: two particles can either remain associated with each other or rebound and remain independent. The association of particles lead to aggregation and induce precipitates formation while the latter, particles remain dispersed in the liquid. Hence peptization is important to disperses the colloidal particles and stabilize the sol (Pierre, 1998). The peptization may introduce positive charge at the surface of particle and establishing double layers around the particle.

The particles are partially protonated which prevent them from undergoing chemical interaction due to electrostatic repulsion (Burgos and Langlet, 1999). During peptization the parameters such as temperature, pH and molar ratio between precursor and acid give effect to the final particle size of the colloid (Van Gestel et al., 2002b). After the process completed, stable sol can be obtained. The corresponding sols contain individual particles surrounded either by steric barrier or an electrical double layer. The barrier is responsible for interparticle repulsion and sol stability. The sol must be free dust and partial gelation. Otherwise, the produced ceramic layer will suffer with pinhole and defect.

2.4.2.2 Organic additive

The organic additive facilitates the adjustment of sol viscosity which resulting more viscous sol at higher amount, subsequently enhances the gel network strength. As the consequences, the stress generated in the film is reduce and prevents crack formation during drying and sintering (Chen et al., 2004). However, the amount of the organic additive must be as small as possible, which is enough to be the adhesive for the sol. The excess amount of the organic additive in the sol may contribute the increase of pore and grain size after sintering process (Sabataityte et al., 2006). Besides the amount, the molecular weight of the organic additive also brings effect to the pore characteristics as well. Large molecular weight of organic additive induced the formation of large void, which indicate the formation of pinhole in the intermediate layer (Van Gestel et al., 2008). The solution of polyvinyl alcohol (PVA) is usually used as the organic additive for titania sol. In order to prevent flocculation of the sol, hydroxypropyl-cellulose (HPC) is necessarily added into PVA solution (Alem et al., 2009a). Table 2.2 shows the combination of titania precursor and the organic binder for the preparation of intermediate layer.

Table 2.2: Titania precursor and organic additive

Titania precursor	Organic additive/molecular weight (g/mol)	References
Tetra isopropyl orthotitanate	HPC/80,000 and PVA/88,000	Alem et al, 2009b
Titanium isopropoxide	HPC/100,000 and PVA/72,000	Van Gestel et al, 2002a
Titanium isopropoxide	HPC/88,000 and PVA/80,000	Ahmad et al, 2010
Titanium butoxide	PVA/72,000	Wong et al, 2003

2.4.2.3 Drying and sintering

Drying process induces the aggregation, gelation and considerable reorganization of the gel structure. The drying gel is called xerogel and aerogel, based on the drying method (Vivier et al., 1998). Multiple cycle of dip-coating – drying – calcination of intermediate layer should be accomplished to repair the defects present in the previous layer. However each ceramic materials having maximum allowable thickness before the layer started to crack. Thus the thickness of the ceramic layer should not be exceeded maximum allowable value. Table 2.3 shows the maximum allowable thickness for certain ceramic materials.

Table 2.3: Maximum allowable ceramic thickness under given conditions

Material	Maximum thickness first dip (μm)	Maximum thickness total (μm)	Sol particle size (nm)	Surface roughness (nm)
$\gamma\text{-Al}_2\text{O}_3$	8	24	40	<300
TiO_2	2	>6	25-30	<100
SiO_2	0.05-0.1	0.05-0.1	0.2-2	40

Sintering temperature play important role in the formation of ceramic material such as titania. The formation of titania begin with amorphous followed by anatase and rutile. The amorphous and rutile are thermodynamically metastable while the rutile is stable. During sintering, the amorphous titania is transform into anatase crystal. At higher sintering temperature, the anatase crystal transformed into rutile which consists of larger crystallite size. The arrangement of large crystallite induces the formation of large pores, which is undesirable in substrate preparation. Meanwhile, the anatase crystal possesses small crystallite size and higher symmetry.

Thus the arrangement of anatase crystal during sintering induce the formation of open structure with high porosity and small pore size (Buchanan and Park, 1997).

During sintering process, the material diffusion occurs and classified into non-densifying and densifying mechanism. Non-densifying mechanism leads to neck growth and coarsening of the particles without densification and shrinkage. Meanwhile, the non-densifying mechanism allows the material to diffuse from the grain boundary to the pores and contribute to neck growth and shrinkage. Figure 2.6 illustrates the neck formation of two particles during initial step of sintering.

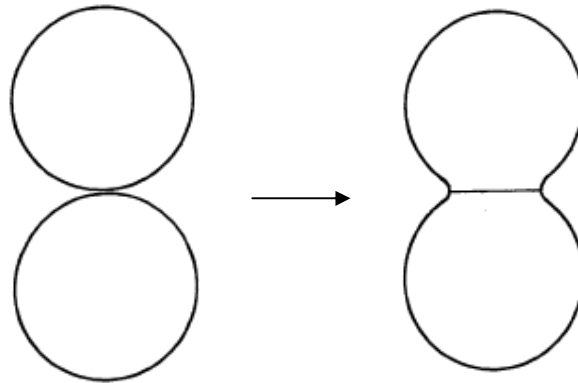


Figure 2.6 Schematic diagram of the neck formation during initial step of sintering

When the sintering temperature reach 0.5 to 0.9 of the melting point, grain boundary diffusion takes place and hence grain growth start to become significant. During this step, small particles which having strong curvature and energy are swallowed by the larger particles. The grain growth leads to the simultaneous growth of the pore size and decrease in the porosity. As a consequence, the pore volume and surface area of the intermediate layer will decrease (Mallada and Menéndez, 2008).

2.4.3 Carbon film

Carbon film is located at the outer surface of CMS membrane. It is the first part of membrane which receives the gas at the feed section of permeation cell. Carbon film acts as the selective layer which responsible for gas separation based on size of the gas molecules.

2.4.3.1 Precursor

The precursor for CMS membrane must exhibit three dimensional crosslink structure. The crosslink structure provide rigidity to the precursor, thus induce to withstand high temperature and prevent liquefies during carbonization (Saufi and Ismail, 2004). The crosslink structure also prevent graphitizing of the precursor during carbonization, thus turn the precursor into non-graphitize carbon (Burket et al., 2008). The thermosetting polymer is usually applied as the precursor of CMS membrane as the structure consists of extensive crosslink. The structure of thermosetting polymer back bone may influence the performance of CMS membrane. The present of aromatic group on the back bone provide high carbon yield after carbonization, which is a good property of CMS membrane precursor. Various types of thermosetting polymers are available in the commercial market such as polyetherimide, polyacrylonitrile, polyimide, phenolic resin, etc. Each thermosetting polymer possesses different kind of structure, indicates various characteristics of the CMS membranes (Tin et al., 2004). Table 2.4 shows the common modification of polymer precursor for CMS membrane.